



Original articles

Research article

<https://doi.org/10.17308/kcmf.2022.24/9266>**Kinetics of the cathodic evolution of hydrogen on alloys of the $\text{Mo}_x\text{W}_{1-x}\text{Si}_2$ system in an alkaline electrolyte**V. V. Panteleeva¹✉, G. A. Simonov¹, A. B. Shein¹, P. A. Miloserdov², V. A. Gorshkov²¹Perm State University,

15 Bukirev str., Perm 614990, Russian Federation

²Merzhanov Institute of Structural Macrokinetics and Materials Science, Russian Academy of Sciences,

8 Academician Osipyan str., Chernogolovka 142452, Russian Federation

Abstract

The kinetics and mechanism of the hydrogen evolution reaction on alloys of the $\text{Mo}_x\text{W}_{1-x}\text{Si}_2$ system ($x = 1.0; 0.68; 0.41; 0$) in a 1.0 M NaOH solution have been studied by the methods of polarization and impedance measurements. The cathodic polarization curves of silicides were characterized by the Tafel plots with constants a and b , equal to 0.47–0.49 and 0.068–0.076 V, respectively. The impedance spectra of $\text{Mo}_x\text{W}_{1-x}\text{Si}_2$ electrodes in the Tafel region are a combination of a capacitive semicircle with a displaced centre at high frequencies and an inductive arc at low frequencies. In the region of the highest frequencies on the impedance plots a straight-line section with a slope slightly higher than 45° was recorded, indicating the presence of pores in the surface layer of the electrodes.

To describe the hydrogen evolution reaction on silicides an equivalent electrical circuit was used, the Faraday impedance of which consisted of series-connected charge transfer resistance R_1 and a parallel R_2C_2 -chain (at $R_2 < 0$, $C_2 < 0$), which corresponded to the atomic hydrogen adsorption on the electrode surface. The impedance of the double layer capacitance was modelled by the constant phase element CPE₁.

The results of polarization and impedance measurements for the investigated silicides were in satisfactory agreement with the discharge – electrochemical desorption mechanism, in which both stages are irreversible and have unequal transfer coefficients. The limiting stage is the electrochemical desorption. The Langmuir isotherm for adsorbed atomic hydrogen was fulfilled. It was concluded that $\text{Mo}_x\text{W}_{1-x}\text{Si}_2$ alloys in an alkaline electrolyte are promising electrode materials that are active in the electrolytic hydrogen evolution reaction.

Keywords: Molybdenum and tungsten silicides, Hydrogen evolution reaction, Electrocatalysis, Self-propagating high-temperature synthesis

Funding: The research was supported by the Perm Research and Education Centre for Rational Use of Subsoil, 2021 and within the state assignment to Merzhanov Institute of Structural Macrokinetics and Materials Science, Russian Academy of Sciences.

For citation: Panteleeva V. V., Simonov G. A., Shein A. B., Miloserdov P. A., Gorshkov V. A. Kinetics of the cathodic evolution of hydrogen on alloys of the $\text{Mo}_x\text{W}_{1-x}\text{Si}_2$ system in an alkaline electrolyte. *Condensed Matter and Interphases*. 2022;24(2): 256–264. <https://doi.org/10.17308/kcmf.2022.24/9266>

Для цитирования: Пантелеева В. В., Симонов Г. А., Шеин А. Б., Милосердов П. А., Горшков В. А. Кинетика катодного выделения водорода на сплавах системы $\text{Mo}_x\text{W}_{1-x}\text{Si}_2$ в щелочном электролите. *Конденсированные среды и межфазные границы*. 2022;24(2): 256–264. <https://doi.org/10.17308/kcmf.2022.24/9266>

✉ Viktoria V. Panteleeva, e-mail: vikpant@mail.ru

© Panteleeva V. V., Simonov G. A., Shein A. B., Miloserdov P. A., Gorshkov V. A., 2022



The content is available under Creative Commons Attribution 4.0 License.

1. Introduction

Among the priority areas for the development of research in the hydrogen energetics, the search for efficient and inexpensive electrode materials for the electrolytic production of hydrogen occupies a leading position. In this regard, metals, alloys, intermetallic and metal-like compounds, and composite materials have been studied as catalysts for the hydrogen evolution reaction of (HER) [1–9]. The study of HER on transition metal silicides showed [1–3, 5–7, 10–14] that the electrocatalytic activity of these materials in the cathodic process depends significantly on the nature and concentration of the metal in the compound, the structure of the material, the pH, and the composition of the medium. A number of authors [2, 5, 11, 14] noted the high electrochemical activity of silicides in HER and the corrosion resistance of these compounds.

Transition metal silicides can be obtained by various methods (direct synthesis from elements, electrolysis of melts, thermal reduction of metal oxides, gas-phase synthesis, etc. [15]). One of the most high-performance and low-power-consuming methods for obtaining silicides and composite materials based on them is self-propagating high-temperature synthesis (SHS) [16]. The use of this method allows controlling the chemical and phase composition, the microstructure of the resulting material by changing the composition of the initial mixture and synthesis parameters.

The aim of this study was to establish the kinetics and mechanism of the reaction of hydrogen evolution on $\text{Mo}_x\text{W}_{1-x}\text{Si}_2$ silicides ($x = 1.0; 0.68; 0.41; 0$) synthesized by the SHS method in an alkaline electrolyte and the determination of the electrochemical activity of $\text{Mo}_x\text{W}_{1-x}\text{Si}_2$ in HER.

2. Experimental

$\text{Mo}_x\text{W}_{1-x}\text{Si}_2$ silicides ($x = 1.0; 0.68; 0.41; 0$), obtained by the SHS method from powder oxides of molybdenum and tungsten (analytical grade) and silicon KR-0 mixed with aluminium in an argon atmosphere under a gas pressure of 5 MPa. The synthesis technique and research materials are described in detail in [17].

For electrochemical measurements, the samples were placed in specially made fluoroplastic holders and filled with polymerised

epoxy resin, leaving only the working surface of the electrodes uninsulated, which was 0.8–1.4 cm². All the specific values provided in the study are presented per unit of the geometric area of the electrode surface. Before measurements, the electrode surface was polished with abrasive papers with a successive decrease in grain size, degreased with ethyl alcohol, and rinsed with a working solution.

Electrochemical measurements were carried out at a temperature of 25 °C under natural aeration conditions in an unstirred 1.0 M NaOH solution. The solution was prepared using deionized water (water resistivity, 18.2 MΩ cm, organic carbon content, 4 µg/L), obtained using a Milli-Q water purification system from Millipore (France), and NaOH (chemically pure).

The measurements were carried out using a potentiostat-galvanostat with a built-in Solartron 1280C frequency analyser (Solartron Analytical, Great Britain) in an YASE-2 electrochemical cell with cathode and anode sections separated by a porous glass diaphragm. A saturated silver chloride electrode was used as the reference electrode and a platinum electrode was used as the auxiliary electrode. The potentials in the study are presented relative to the standard hydrogen electrode.

Once the electrode was immersed in the solution, it was subjected to cathodic polarisation with a current density of 0.5 mA/cm² within 10 min; then held with an open circuit potential until a stable potential was established, which was -0.63 ± 0.02 , -0.66 ± 0.02 , -0.69 ± 0.03 and -0.80 ± 0.02 V for MoSi_2 -, $\text{Mo}_{0.68}\text{W}_{0.32}\text{Si}_2$ -, $\text{Mo}_{0.41}\text{W}_{0.59}\text{Si}_2$ -, and WSi_2 electrodes, respectively; then the impedance spectra were recorded. Before the measurement of the impedance spectra, potentiostatic polarisation of the electrode was conducted at each potential until an almost constant current value was established. After that, the impedance was measured at this value of E and lower potentials, and the potential was changed with a fixed step. Cathodic potentiostatic curves were plotted based on the obtained values of i values for a given value of E . The range of frequencies used for impedance measurements $f(\omega/2\pi)$ was from 20 kHz to 0.01 Hz (10 points per decade with a uniform distribution on a logarithmic scale), the amplitude of the alternating signal was 5–10 mV.

The value of hydrogen evolution overvoltage was determined relative to the equilibrium potential of the hydrogen electrode in a 1.0 M NaOH solution (-0.818 V).

The data were measured and processed using the programs CorrWare2, ZPlot2, and ZView2 (Scribner Associates, Inc.). Confidence intervals were calculated at a significance level of 0.05.

3. Results and discussion

The cathodic polarization curves of MoSi_2 -, $\text{Mo}_{0.68}\text{W}_{0.32}\text{Si}_2$ -, $\text{Mo}_{0.41}\text{W}_{0.59}\text{Si}_2$ -, and WSi_2 electrodes corrected for the Ohmic drop [18] in a 1.0 M NaOH solution are shown in Fig. 1.

The cathodic curves of MoSi_2 , $\text{Mo}_{0.68}\text{W}_{0.32}\text{Si}_2$, and $\text{Mo}_{0.41}\text{W}_{0.59}\text{Si}_2$ silicides had the same type and were characterized by the presence of a Tafel region in the potential range from -1.04 to -1.13 V with a slope $b \approx 0.068$ – 0.074 V and constant a equal to ~ 0.47 – 0.49 V (Table 1). The polarisation curve of the WSi_2 electrode had a linear section in the potential range from -1.0 to -1.1 V with a slope of ~ 0.076 V and $a \approx 0.48$ V (Table 1). Based on the constant values a and b in accordance with [19], it was concluded that the studied silicides in an alkaline electrolyte are materials with a low overvoltage for hydrogen evolution.

The theoretical value of the Tafel slope was ~ 0.06 V (with transfer the coefficients of $\alpha \approx 0.5$ for charge transfer stages), the values of b were

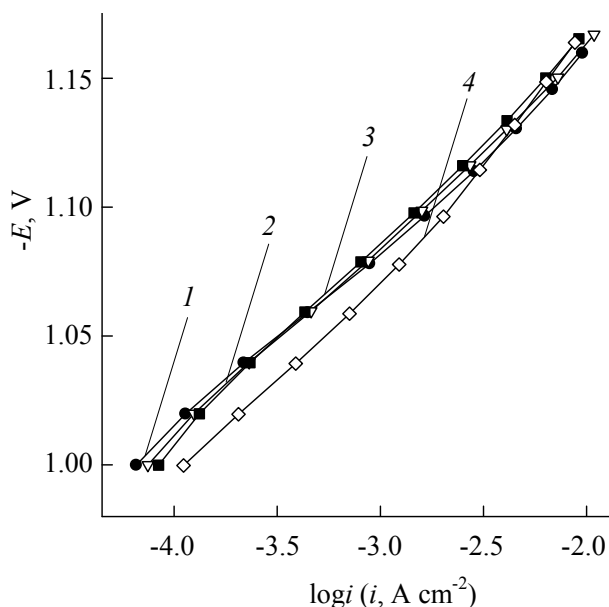


Fig. 1. Cathodic polarization curves in 1.0 M NaOH: 1 – MoSi_2 ; 2 – $\text{Mo}_{0.68}\text{W}_{0.32}\text{Si}_2$; 3 – $\text{Mo}_{0.41}\text{W}_{0.59}\text{Si}_2$; 4 – WSi_2

closest when reordered for $\text{Mo}_x\text{W}_{1-x}\text{Si}_2$ electrodes (Table 1) may have several explanations. Tafel slope ~ 0.06 V can be observed in the case of following mechanisms, assuming that the Langmuir adsorption isotherm for adsorbed atomic hydrogen H_{ads} was fulfilled: 1) delayed barrier-free discharge or delayed barrier-free electrochemical desorption [20]; 2) delayed surface diffusion of atomic hydrogen (for this mechanism, the Tafel slope is ~ 0.06 V [21] or ~ 0.079 V [22]).

The value of b of ~ 0.06 V when the logarithmic Temkin adsorption isotherm for H_{ads} was fulfilled, can be explained in the case of following mechanisms [23]: 1) discharge – recombination with a quasi-equilibrium discharge stage with non-activated hydrogen adsorption; 2) discharge – electrochemical desorption with a quasi-equilibrium discharge stage.

The observed relatively small deviations of the Tafel slope for $\text{Mo}_x\text{W}_{1-x}\text{Si}_2$ from the theoretical ~ 0.06 V can be associated with specific values of the transfer coefficients of HER stages and other factors [24].

For the clarification of the mechanism and kinetic regularities of HER on silicides, the frequency dependences of the impedance components were measured.

The impedance spectra of $\text{Mo}_x\text{W}_{1-x}\text{Si}_2$ silicides for all studied values of E were a combination of a capacitive semicircle with a centre below the axis of the real component of the impedance Z' at high frequencies (HF) and the inductive arc at low frequencies (Fig. 2). On the impedance graphs in the region of the highest frequencies, deviations from the semicircle were recorded. These deviations had the form of almost rectilinear segments with an inclination somewhat higher than 45° and, probably, indicate the presence of pores, approximately corresponding to the model of cylindrical pores in the surface layer of

Table 1. Kinetic parameters of the hydrogen evolution reaction on the alloys of the $\text{Mo}_x\text{W}_{1-x}\text{Si}_2$ system in 1.0 M NaOH

Electrode	$-b, \text{V}$	$-a, \text{V}$
MoSi_2	0.068 ± 0.001	0.47 ± 0.01
$\text{Mo}_{0.68}\text{W}_{0.32}\text{Si}_2$	0.071 ± 0.001	0.48 ± 0.01
$\text{Mo}_{0.41}\text{W}_{0.59}\text{Si}_2$	0.074 ± 0.002	0.49 ± 0.02
WSi_2	0.076 ± 0.001	0.48 ± 0.02

the electrodes [25]. The slope angle higher than 45° can be explained by the significant influence of the “flat” electrode surface around the pores [26], for which the slope Z'' , Z' -dependences in the high frequency region was lower than 90° , but significantly higher than 45° (see below the data for the CPE constant phase element). Resistance R_Ω , equal to the distance between the point obtained by extrapolation of the rectilinear section to the region of high frequencies to the intersection with the axis Z' , and the point obtained by extrapolating the capacitive semicircle into the HF-region to the intersection with the axis Z' , was 0.44 ± 0.02 , 0.46 ± 0.02 , 0.41 ± 0.03 , and $0.47 \pm 0.02 \text{ } \Omega \cdot \text{cm}^2$ for MoSi_2 -, $\text{Mo}_{0.68}\text{W}_{0.32}\text{Si}_2$ -, $\text{Mo}_{0.41}\text{W}_{0.59}\text{Si}_2$ -, and WSi_2 electrodes, respectively. The low value of R_w indicated that the pores were not deep.

According to the theory of porous electrodes for the model of cylindrical pores [27]:

$$R_\Omega = \frac{\rho L}{3n\pi r^2},$$

where r is the resistivity of the electrolyte solution, r and L are the pore radius and length, respectively, n is the number of pores per 1 cm^2 of the electrode surface; $S = n\pi r^2$ is the total cross section of pores per 1 cm^2 of the surfaces. The ratio for R_Ω does not allow to determine r and L separately; only L/r^2 or L/S ratios can be determined. For 1.0 M NaOH , $r = 6.05 \text{ } \Omega \cdot \text{cm}$ [28], and, for example, for the MoSi_2 electrode the L/S ratio

was 0.22 cm^{-1} ; based on the assumption that $S = 0.01 \text{ cm}^2$ we get $L = 22 \text{ } \mu\text{m}$.

Let f_0 denote the frequency corresponding to the transition point from a rectilinear HF section to a capacitive semicircle. At the frequency f_0 the alternating current passes through the entire length of the pores, and at $f < f_0$ the electrode with pores behaves like a smooth electrode with a surface area equal to the total surface of the electrode, including the inner surface of the pores [26]. For the processing of the impedance spectra for the study of the kinetics and mechanism of HER, points at $f < f_0$ were selected. This allows the use of equivalent circuits normally used for smooth electrodes.

The impedance graphs of $\text{Mo}_x\text{W}_{1-x}\text{Si}_2$ electrodes indicate the staged nature of HER. At least two time constants were required for the description. The registration of the inductive impedance in the low-frequency region indicates that HER proceeded according to the discharge-electrochemical desorption path. According to [29], the inductive impedance can appear only when H_{ads} is removed via the electrochemical desorption stage and cannot appear in the case of the discharge-recombination mechanism. Thus, based on the frequency dependences of the impedance components, it can be concluded that in the studied range of potentials for the description of hydrogen evolution on the $\text{Mo}_x\text{W}_{1-x}\text{Si}_2$ silicides discharge - recombination path can be rejected.

The equivalent electrical circuits shown in Fig. 3 were used for the modelling of HER on

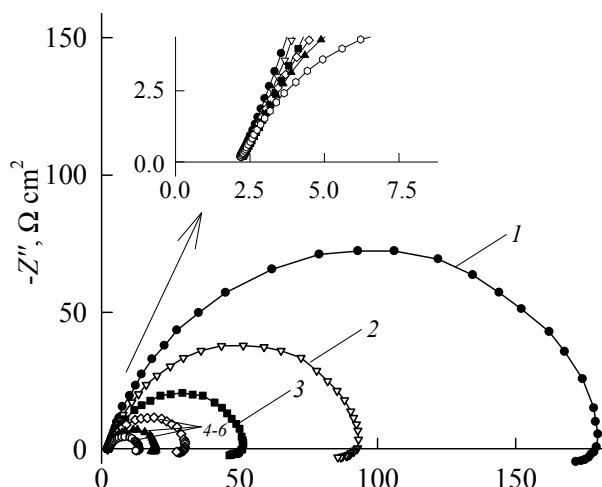


Fig. 2. Impedance spectra of MoSi_2 in 1.0 M NaOH at $E, \text{ V}$: 1 – -1.04 ; 2 – -1.06 ; 3 – -1.08 ; 4 – -1.10 ; 5 – -1.12 ; 6 – -1.14

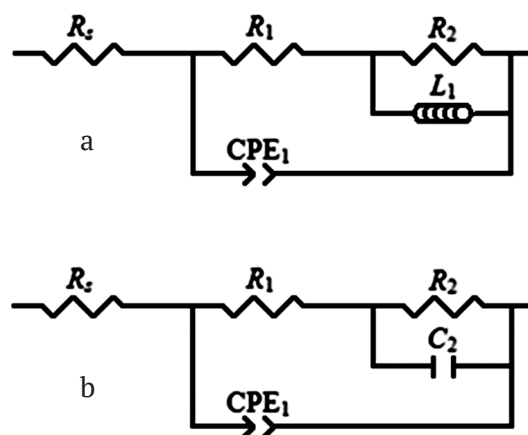


Fig. 3. Equivalent electrical circuits for the alloys of the $\text{Mo}_x\text{W}_{1-x}\text{Si}_2$ system in 1.0 M NaOH in the range of potentials of hydrogen evolution

$\text{Mo}_x\text{W}_{1-x}\text{Si}_2$ silicides. In the diagram shown in Fig. 3a: R_s is the electrolyte resistance, R_1 is the polarization resistance, resistance R_2 and inductance L_1 describe the atomic hydrogen adsorption (filling relaxation of H_{ads} when an alternating signal is applied) on the electrode surface, the CPE_1 element simulates double layer capacitance on the inhomogeneous surface of the solid electrode.

The impedance of the constant phase element is:

$$Z_{\text{CPE}} = Q^{-1}(j\omega)^{-p}.$$

In this ratio, with $p = 1 - \gamma$ the constant phase element is non-ideal capacitance; γ is the value significantly less than 1 (typically $\gamma < 0.2$) [18].

The equivalent circuit in Fig. 3b is identical to the circuit in Fig. 3a (in the scheme in Fig. 3b: R_1 is the charge transfer resistance, and the adsorption of atomic hydrogen on the electrode surface is modelled using the R_2C_2 -chain). According to [30], to describe HER on electrodes that correspond to impedance spectra with inductance in the low-frequency region, it is advisable to use the equivalent circuit in Fig. 3b with negative R_2 and C_2 . In this case, absolute values of $|R_2|$ and $|C_2|$ are used as diagnostic criteria for HER mechanisms based on the analysis of the dependence of the Faraday impedance parameters on the potential.

Experimental impedance spectra of silicides at the studied values of E were satisfactorily described by the diagram in Fig. 3b with negative values of R_2 and C_2 . The criterion χ^2 calculated by ZView2 (using statistical weights expressed via the reciprocal of the impedance module) was $(1.1\text{--}2.3) \cdot 10^{-4}$; the sum of square deviations was $(1.0\text{--}2.1) \cdot 10^{-2}$; the error in determining the values R_s, R_1 , and CPE_1 did not exceed 1–3%, and reached 8–10% for the parameters R_2 and C_2 . Parameter

values of the equivalent circuit for the MoSi_2 electrode are shown in Table 2.

The results of the determination of the numerical values of $X = R_1, |R_2|, |C_2|$ parameters of the equivalent circuit in Fig. 3b for $\text{Mo}_x\text{W}_{1-x}\text{Si}_2$ electrodes were analysed depending on the potential in semilogarithmic coordinates. $\lg X, E$ dependencies for the MoSi_2 electrode, corrected for the ohmic potential drop are shown in Fig. 4. The slopes $(\partial \lg X / \partial E)_{c_{\text{NaOH}}}$ for $\text{Mo}_x\text{W}_{1-x}\text{Si}_2$ are shown in Table 3. For all the studied silicides at the potentials of the Tafel region, a linear decrease in the values of $\lg R_1$ and $\lg |R_2|$ and a weak increase in $\lg |C_2|$ with increasing cathodic polarization were revealed.

Based on the polarization measurements, for HER on silicides was considered the mechanism of discharge–electrochemical desorption with a quasi-equilibrium stage of the discharge when

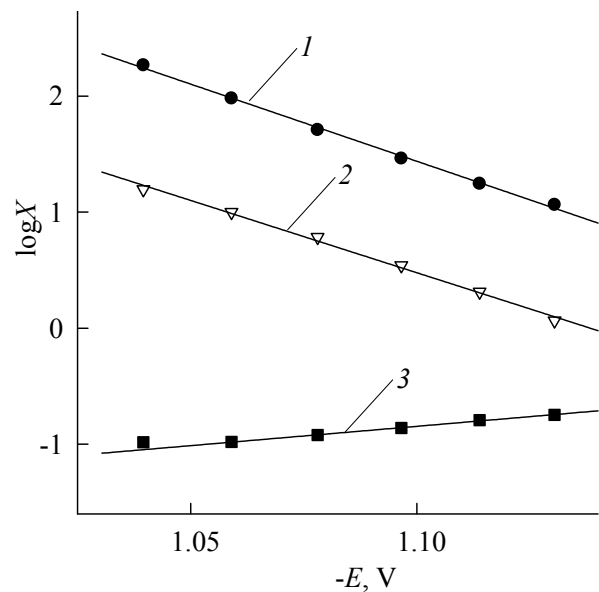


Fig. 4. Dependences of $\log X$ (X : 1 – R_1 , 2 – $|R_2|$, 3 – $|C_2|$) on the potential of MoSi_2 in 1.0 M NaOH. Values of R_1 and R_2 are in $\text{W}\cdot\text{cm}^2$, C_2 in $\text{F}\cdot\text{cm}^{-2}$

Table 2. The values of the equivalent electrical circuit (Fig. 3b) parameters for MoSi_2 in 1.0 M NaOH

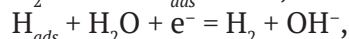
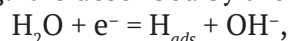
$-E, \text{V}$	$R_1, \Omega\cdot\text{cm}^2$	$R_2, \Omega\cdot\text{cm}^2$	$-C_2, \text{F}\cdot\text{cm}^{-2}$	$Q_1\cdot 10^4, \text{F}\cdot\text{cm}^{-2}\cdot\text{s}^{(p_1-1)}$	p_1
1.04	184.9	15.8	0.104	4.69	0.827
1.06	95.8	10.0	0.105	4.82	0.831
1.08	51.2	6.1	0.120	4.89	0.834
1.10	29.0	3.5	0.138	4.89	0.842
1.12	17.6	2.0	0.161	4.74	0.858
1.14	11.6	1.2	0.179	5.19	0.852

the logarithmic adsorption isotherm for H_{ads} was fulfilled. However, for this mechanism, in accordance with [30] the independence of R_1 and C_2 from the potential was noted. The significant decrease in R_1 and the small increase in $|C_2|$ with the potential (Table 2) experimentally registered for $\text{Mo}_x\text{W}_{1-x}\text{Si}_2$ silicides did not correspond to the theoretical ones for the considered HER mechanism.

The mechanism of slow surface diffusion of atomic hydrogen during hydrogen evolution on $\text{Mo}_x\text{W}_{1-x}\text{Si}_2$ silicides can be considered probable, since different atoms are present in the studied materials, and, consequently, the formation of adsorbed hydrogen atoms during the transfer of an electron to a water molecule and electrochemical desorption H_{ads} can occur on different parts of the surface (active centres) of the electrodes. The use of an equivalent circuit corresponding to this mechanism [31] for modelling the impedance spectra of silicides leads to high errors in determining the diffusion impedance parameters and capacitance values for H_{ads} on active sites to which surface diffusion occurs. Probably, the mechanism of delayed surface diffusion can also be rejected.

Parallel $\lg R_1, E$ - and $\lg |R_2|, E$ -dependencies and a slight change in $\lg |C_2|$ with decreasing potential are characteristic of the discharge – electrochemical desorption mechanism, in which both stages are irreversible and the transfer coefficients of the stages are not equal [30]. The impedance measurements were carried out at an overvoltage higher than 0.18 V, which are sufficiently high for the stages to be irreversible. According to [30], in this mechanism, with a logarithmic adsorption isotherm for H_{ads} there is no inductance on the impedance spectra. In the case of the Langmuir isotherm, inductance

can appear both in the case of a slow stage of the discharge and in the case of a slow stage of electrochemical desorption. Thus, based on the obtained dependences of the elements of the Faraday impedance of $\text{Mo}_x\text{W}_{1-x}\text{Si}_2$ electrodes from E it can be assumed that HER on silicides in the studied potential range proceeds according to the discharge - electrochemical desorption path, e.g. it is described by the sequence of reactions:



with the Langmuir adsorption isotherm for H_{ads} . Additional criteria for HER mechanisms based on dependency analysis of iR_1 , $|iR_2|$, and R_2C_2 on the electrode potential [32], also indicate the implementation of this mechanism on silicides. For MoSi_2 the electrode slopes $(\partial \lg Y / \partial E)_{c_{\text{NaOH}}}$ for $Y = iR_1, |iR_2|, R_2C_2$ were -1.3 ± 0.2 , -1.1 ± 0.4 , and $9.8 \pm 0.4 \text{ V}^{-1}$ respectively.

With irreversible stages of HER there are two possible explanations for the results obtained: a) the limiting stage is the formation of H_{ads} with the transfer of an electron to a H_2O molecule $\alpha_1 > \alpha_2$; b) the limiting step is electrochemical desorption, $\alpha_1 < \alpha_2$. Here α_1 and α_2 are the transfer coefficients of the discharge and electrochemical desorption stages, respectively. Molybdenum and tungsten are metals with a very high binding energy with hydrogen $E_{\text{M-H}}$ [20]. In this case, $E_{\text{W-H}}$ was about 12 kJ/mol higher than $E_{\text{Mo-H}}$ during adsorption from the gas phase, and estimates for aqueous solutions provide close $E_{\text{M-N}}$ values for these metals. Due to the high strength of the metal-hydrogen bond, the probable mechanism of HER for Mo and W in acidic solutions is delayed electrochemical desorption (barrier-free at relatively low η and ordinary at higher η) [20]. Probably, $E_{\text{M-N}}$ on molybdenum and tungsten silicides is somewhat different from $E_{\text{M-N}}$ for pure

Table 3. The values of $(\partial \lg X / \partial E)_{c_{\text{NaOH}}}$ ($X = R_1, |R_2|, |C_2|$) slopes and transfer coefficients α_1 and α_2 for the alloys of the $\text{Mo}_x\text{W}_{1-x}\text{Si}_2$ system in 1.0 M NaOH

Electrode	$\left(\frac{\partial \lg R_1}{\partial E}\right)_{c_{\text{NaOH}}}, \text{V}^{-1}$	$\left(\frac{\partial \lg R_2 }{\partial E}\right)_{c_{\text{NaOH}}}, \text{V}^{-1}$	$\left(\frac{\partial \lg C_2 }{\partial E}\right)_{c_{\text{NaOH}}}, \text{V}^{-1}$	α_1	α_2
MoSi_2	13.3 ± 0.2	13.1 ± 0.4	-3.3 ± 0.4	0.59 ± 0.04	0.78 ± 0.02
$\text{Mo}_{0.68}\text{W}_{0.32}\text{Si}_2$	12.9 ± 0.3	12.6 ± 0.3	-3.6 ± 0.2	0.55 ± 0.02	0.76 ± 0.03
$\text{Mo}_{0.41}\text{W}_{0.59}\text{Si}_2$	12.1 ± 0.4	12.3 ± 0.5	-3.8 ± 0.4	0.49 ± 0.04	0.72 ± 0.04
WSi_2	10.5 ± 0.2	10.3 ± 0.3	-4.8 ± 0.3	0.34 ± 0.03	0.62 ± 0.02

metals. At the same time, it was shown that the electrocatalytic activity of silicides correlates with the activity of the corresponding metals, and the highest current densities were observed on platinum silicide [3]. It can be assumed that on molybdenum and tungsten silicides, as well as on Mo and W, the hydrogen adsorption energy is high. Therefore, out of the two described above variants, variant (b), which is delayed electrochemical desorption, seems to be more probable. At the same time, this stage is probably in the transition state from ordinary electrochemical desorption to barrier-free desorption, which is expressed as higher α_2 values (Table 3). The HER stage transfer coefficients on $\text{Mo}_x\text{W}_{1-x}\text{Si}_2$ were calculated based on the ratios provided in [30]: the transfer coefficient α_2 of the limiting stage was determined based on the slope of $\lg R_1, E$ -dependencies, and the difference ($\alpha_2 - \alpha_1$) was determined based on the slope of $\lg |C_2|, E$ -dependencies.

4. Conclusions

Based on polarization and impedance measurements, it was shown that the reaction of hydrogen evolution on alloys of $\text{Mo}_x\text{W}_{1-x}\text{Si}_2$ system in an alkaline electrolyte proceeds according to the discharge – electrochemical desorption path with a delayed stage of electrochemical desorption, both stages were irreversible, and the transfer coefficients of the stages were not equal. The Langmuir isotherm for adsorbed atomic hydrogen was fulfilled. It was found that alloys of the $\text{Mo}_x\text{W}_{1-x}\text{Si}_2$ system in an alkaline electrolyte are characterized by a low overvoltage of hydrogen evolution and, thus, represent promising electrode materials for the electrolytic production of hydrogen.

Author contributions

All authors made an equivalent contribution to the preparation of the publication.

Conflict of interests

The authors declare that they have no known competing financial interests or personal relationships that could have influenced the work reported in this paper.

References

1. Shamsul Huq A. K. M., Rosenberg A. J. J. Electrochemical behavior of nickel compounds: I. The

hydrogen evolution reaction on NiSi, NiAs, NiSb, NiS, NiTe₂, and their constituent elements. *Journal of The Electrochemical Society*. 1964;111(3): 270-278. <https://doi.org/10.1149/1.2426107>

2. Tilak B. V., Ramamurthy A. C., Conway B. E. High performance electrode materials for the hydrogen evolution reaction from alkaline media. *Proceedings of the Indian Academy of Sciences – Chemical Sciences volume*. 1986;97(3-4): 359–393. <https://doi.org/10.1007/BF02849200>

3. Wirth S., Harnisch F., Weinmann M., Schröder U. Comparative study of IVB–VIB transition metal compound electrocatalysts for the hydrogen evolution reaction. *Applied Catalysis B: Environmental*. 2012;126: 225–230. <https://doi.org/10.1016/j.apcatb.2012.07.023>

4. Meyer S., Nikiforov A. V., Petrushina I. M., Kohler K., Christensen E., Jensen J. O., Bjerrum N. J. Transition metal carbides (WC, Mo₂C, TaC, NbC) as potential electrocatalysts for the hydrogen evolution reaction (HER) at medium temperatures. *International Journal of Hydrogen Energy*. 2015;40(7): 2905–2911. <https://doi.org/10.1016/j.ijhydene.2014.12.076>

5. Safizadeh F., Ghali E., Houlachi G. Electrocatalysis developments for hydrogen evolution reaction in alkaline solutions – A Review. *International Journal of Hydrogen Energy*. 2015;40(1): 256–274. <https://doi.org/10.1016/j.ijhydene.2014.10.109>

6. Sapountzi F. M., Gracia J. M., Weststrate C. J., Fredriksson H. O. A., Niemantsverdriet J. W. Electrocatalysts for the generation of hydrogen, oxygen and synthesis gas. *Progress in Energy and Combustion Science*. 2017;58: 1–35. <https://doi.org/10.1016/j.pecs.2016.09.001>

7. Eftekhari A. Electrocatalysts for hydrogen evolution reaction. *International Journal of Hydrogen Energy*. 2017;42(16): 11053–11077. <https://doi.org/10.1016/j.ijhydene.2017.02.125>

8. Kichigin V. I., Shein A. B. An electrochemical study of the hydrogen evolution reaction at YNi₂Ge₂ and LaNi₂Ge₂ electrodes in alkaline solutions. *Journal of Electroanalytical Chemistry*. 2018;830-831: 72–79. <https://doi.org/10.1016/j.jelechem.2018.10.029>

9. Theerthagiri J., Lee S. J., Murthy A. P., Madhavan J., Choi M. Y. Fundamental aspects and recent advances in transition metal nitrides as electrocatalysts for hydrogen evolution reaction: A review. *Current Opinion in Solid State and Materials Science*. 2020;24(1): 100805–100827. <https://doi.org/10.1016/j.cossms.2020.100805>

10. Vijh A. K., Belanger G., Jacques R. Electrochemical activity of silicides of some transition metals for the hydrogen evolution reaction in acidic solutions. *International Journal of Hydrogen Energy*. 1990;15(11): 789–794. [https://doi.org/10.1016/0360-3199\(90\)90014-P](https://doi.org/10.1016/0360-3199(90)90014-P)

11. Vijn A. K., Belanger G., Jacques R. Electrolysis of water on silicides of some transition metals in alkaline solutions. *International Journal of Hydrogen Energy*. 1992;15(7): 479–483. [https://doi.org/10.1016/0360-3199\(92\)90146-N](https://doi.org/10.1016/0360-3199(92)90146-N)
12. Kichigin V. I., Shein A. B. Kinetics and mechanism of hydrogen evolution reaction on cobalt silicides in alkaline solutions. *Electrochimica Acta*. 2015;164: 260–266. <https://doi.org/10.1016/j.electacta.2015.02.198>
13. Panteleeva V. V., Votinov I. S., Polkovnikov I. S., Shein A. B. Kinetics of cathodic hydrogen evolution manganese monosilicide in sulfuric acid electrolyte. *Kondensirovannye sredy i mezhfaznye granitsy = Condensed Matter and Interphases*. 2019;21(3): 432–440. (In Russ., abstract in Eng.). <https://doi.org/10.17308/kcmf.2019.21/1153>
14. Kuzminykh M. M., Panteleeva V. V., Shein A. B. Cathodic hydrogen evolution on iron disilicide. I. Alkaline solution. *Izvestiya vuzov. Khimiya i khimicheskaya tekhnologiya = ChemChemTech*. 2019;62(1): 38–45. <https://doi.org/10.6060/ivkkt.20196201.5745>
15. Gurin V. N. Methods for the preparation of refractory compounds of transition metals and prospects for their development. *Uspekhi khimii = Russian Chemical Reviews*. 1972;41(4): 323–340. <https://doi.org/10.1070/RC1972v041n04ABEH002059>
16. Merzhanov A. G., Borovinskaya I. P. Self-propagating high-temperature synthesis of refractory inorganic compounds. *Doklady AN SSSR*. 1972;204(2): 366–369. (In Russ.). Available at: http://www.ism.ac.ru/handbook/1st_art.htm
17. Gorshkov V. A., Yukhvid V. I., Miloserdov P. A., Sachkova N. V. Autowave synthesis of cast Mo-W-Si silicides. *Inorganic Materials*. 2011;47(4): 375–378. <https://doi.org/10.1134/S002016851104011X>
18. Orazem M. E., Tribollet B. *Electrochemical impedance spectroscopy*. John Wiley and Sons, Hoboken; 2008. 533 p.
19. Conway B. E., Bai L., Sattar M. A. Role of the transfer coefficient in electrocatalysis: applications to the H_2 and O_2 evolution reactions and the characterization of participating adsorbed intermediates. *International Journal of Hydrogen Energy*. 1987;12(9): 607–621. [https://doi.org/10.1016/0360-3199\(87\)90002-4](https://doi.org/10.1016/0360-3199(87)90002-4)
20. Krishtalik L. I. Hydrogen overvoltage and adsorption phenomena: Part III. Effect of the adsorption energy of hydrogen on overvoltage and the mechanism of the cathodic process. In: P. Delahay (Ed.), *Advances in Electrochemistry and Electrochemical Engineering*. Vol. 7. Intersci. Publ., New York; 1970. pp. 283–340.
21. Fleischmann M., Grenness M. Electrocrystallization of Ruthenium and Electrocatalysis of Hydrogen Evolution. *Journal of the Chemical Society, Faraday Transactions 1: Physical Chemistry in Condensed Phases*. 1972;68: 3205–3215. <https://doi.org/10.1039/F19726802305>
22. Vvedenskii A. V., Gutorov I. A., Morozova N. B. The kinetics of cathodic hydrogen evolution on transition metals. I. Theoretical analysis. *Kondensirovannye sredy i mezhfaznye granitsy = Condensed Matter and Interphases*. 2010;12(3): 288–300. (In Russ., abstract in Eng.). Available at: <https://elibrary.ru/item.asp?id=15574174>
23. Thomas J. G. N. Kinetics of electrolytic hydrogen evolution and the adsorption of hydrogen by metals. *Transactions Faraday Society*. 1961;57(9): 1603–1611. <https://doi.org/10.1039/TF9615701603>
24. Frumkin A. N. *Selected proceedings: hydrogen overvoltage*. Moscow: Nauka Publ.; 1988. 240 p. (in Russ.)
25. Keiser H., Beccu K. D., Gutjahr M. A. Abschätzung der Porenstruktur porösen Elektroden aus Impedanzmessung. *Electrochimica Acta*. 1976;21(8): 539–543. [https://doi.org/10.1016/0013-4686\(76\)85147-X](https://doi.org/10.1016/0013-4686(76)85147-X)
26. Lasia A. Modeling of impedance of porous electrode. In: *Modern Aspects of Electrochemistry*. No. 43. Ed. by M. Schlesinger. Springer, New York, 2009. pp. 67–137.
27. Candy J.-P., Fouilloux P., Keddou M., Takenouti H. The characterization of porous electrodes by impedance measurements. *Electrochimica Acta*. 1981;26(8): 1029–1034. [https://doi.org/10.1016/0013-4686\(81\)85072-4](https://doi.org/10.1016/0013-4686(81)85072-4)
28. Sukhotin A. M. *Handbook of electrochemistry*. Leningrad: Khimiya Publ.; 1981. 488 p. (in Russ.)
29. Novoselskii I. M., Gudina N. N. Calculation of the mechanism and kinetics of hydrogen evolution from impedance measurements. *Elektrokhimiya = Soviet Electrochemistry*. 1969;5(6): 670–676. (In Russ.)
30. Kichigin V. I., Shein A. B. Diagnostic criteria for hydrogen evolution mechanisms in electrochemical impedance spectroscopy. *Electrochimica Acta*. 2014;138: 325–333. <https://doi.org/10.1016/j.electacta.2014.06.114>
31. Kichigin V. I., Shein A. B. The kinetics of cathodic hydrogen evolution on CeCu_2Ge_2 electrode in alkaline solution. The role of surface and bulk diffusion of atomic hydrogen. *Bulletin of Perm University. Chemistry*. 2016;23(3): 6–19. (In Russ., abstract in Eng.). Available at: <https://elibrary.ru/item.asp?id=27128572>
32. Kichigin V. I., Shein A. B. Additional criteria for the mechanism of hydrogen evolution reaction in the impedance spectroscopy method. *Bulletin of Perm University. Chemistry*. 2018;8(3): 316–324. (In Russ., abstract in Eng.). <https://doi.org/10.17072/2223-1838-2018-3-316-324>

Information about the authors

Viktoria V. Panteleeva, Cand. Sci. (Chem.), Associate Professor, Department of Physical Chemistry, Perm State University (Perm, Russian Federation).

<https://orcid.org/0000-0002-1506-6665>
vikpant@mail.ru

Grigoriy A. Simonov, Student, Department of Physical Chemistry, Perm State University (Perm, Russian Federation).

<https://orcid.org/0000-0002-9948-6797>
grisha.simonov@yandex.ru

natoliy B. Shein, Dr. Sci. (Chem.), Professor, Head of the Department of Physical Chemistry, Perm State University (Perm, Russian Federation).

<https://orcid.org/0000-0002-2102-0436>
ashein@psu.ru

Pavel A. Miloserdov, Cand. Sci. (Tech.), PhD in Technical Sciences, Senior Researcher, Laboratory for SHS melts and cast materials, Merzhanov Institute of Structural Macrokinetics and Materials Science, Russian Academy of Sciences (Chernogolovka, Russian Federation).

<https://orcid.org/0000-0002-2587-0067>
yu_group@ism.ac.ru

Vladimir A. Gorshkov, Dr. Sci. (Tech.), Leading Researcher, Laboratory for SHS melts and cast materials, Merzhanov Institute of Structural Macrokinetics and Materials Science, Russian Academy of Sciences (Chernogolovka, Russian Federation).

<https://orcid.org/0000-0001-8845-4717>
gorsh@ism.ac.ru

Received 20.10.2021; approved after reviewing 18.02.2022; accepted for publication 15.04.2022; published online 25.06.2022.

Translated by Valentina Mittova

Edited and proofread by Simon Cox